

Modified Regge Calculus as an Explanation of Dark Matter

W.M. Stuckey*

*Department of Physics
Elizabethtown College
Elizabethtown, PA 17022*

Timothy McDevitt

*Department of Mathematical Sciences
Elizabethtown College
Elizabethtown, PA 17022*

Michael Silberstein

*Department of Philosophy
Elizabethtown College
Elizabethtown, PA 17022 and
Department of Philosophy
University of Maryland
College Park, MD 20742*

(Dated: June 1, 2022)

According to modified Regge calculus (MORC), large-scale rarified distributions of matter can lead to perturbative corrections of the corresponding spacetime geometry of general relativity (GR). It is well known in GR that the dynamic mass of the matter generating the exterior Schwarzschild vacuum solution to Einstein's equations can differ from the proper mass of that same matter per the interior solution. For galactic rotation curves and the mass profiles of X-ray clusters, we use MORC to propose that it is precisely this type of mass difference on an enhanced scale that is currently attributed to non-baryonic dark matter. We argue that this same approach is applicable to Regge calculus cosmology and the modeling of anisotropies in the angular power spectrum of the CMB due to acoustic oscillations, so it should be applicable to explaining dark matter phenomena on that scale as well. We account for the value of the dynamic mass by a simple geometric scaling of the proper mass of the baryonic matter in galaxies and galaxy clusters. Since modified Newtonian dynamics (MOND) has been successful in fitting galactic rotation curves without non-baryonic dark matter, we compare our MORC fits to MOND fits of galactic rotation curves data (THINGS). Similarly, metric skew-tensor gravity (MSTG) has been successful explaining the mass profiles of X-ray clusters without non-baryonic dark matter, so we compare our MORC fits to MSTG fits of X-ray cluster data (ROSAT and ASCA). Overall, we find the MORC fits to be comparable to those of MOND and MSTG. Since the MORC approach to the dark matter problem can be extended to cosmology and we already used it to explain dark energy phenomena without accelerating expansion or a cosmological constant, dark matter and dark energy phenomena may simply reflect geometric perturbations to idealized spacetime structure on large scales.

PACS: 95.35.+d; 95.30.Sf; 04.90.+e

Keywords: dark matter, THINGS, MOND, metric skew-tensor gravity, Relational Blockworld, Regge calculus

I. INTRODUCTION

Since the early 1930's, galactic rotation curves (RC's) and galaxy cluster masses have been known to deviate from Newtonian expectations based on luminous matter and known mass-to-luminosity ratios[1–4]. These are two aspects of the dark matter problem[5], making this one of the most persistent problems in physics. As a consequence, many approaches have been brought to bear on the dark matter problem, typically by way of new particles[6, 7], but also by way of modifications to existing theories of gravity, e.g., modified Newtonian dynamics (MOND)[8–10] and relativistic counterparts[11–15],

and Moffat's modified gravity (MOG), i.e., metric skew-tensor gravity (MSTG) and scalar-tensor-vector gravity (STVG)[16, 17]. No one disputes the existence of baryonic dark matter, e.g., brown dwarfs, black holes, and molecular hydrogen, but there is wide agreement that baryonic dark matter does not exist in large enough supply to resolve the dark matter problem[18]. While the assumption of non-baryonic dark matter (DM) in Λ CDM cosmology models works well for explaining cosmological features (scales greater than 1 Mpc), there is still no independent verification of non-baryonic dark matter and galactic RC's do not conform to the theoretical predictions of Λ CDM for the distribution of DM on gravitational scales[19]. Therefore, it is reasonable at this stage to consider modifications to existing theories of gravity that deny the need for DM in resolving the

* stuckeym@etown.edu

dark matter problem. Accordingly, we explain galactic RC's and the mass profiles of X-ray clusters without DM based on our foundations-driven approach to fundamental physics called Relational Blockworld (RBW). We extend this reasoning to cosmological scales, but an RBW fit of anisotropies in the angular power spectrum of the cosmic microwave background (CMB) due to acoustic oscillations remains to be done.

RBW was originally conceived as an interpretation of quantum mechanics[20–22], but it quickly became apparent that it has implications for quantum gravity, unification and astrophysics[23, 24]. According to RBW, reality is fundamentally discrete, so although the lattice geometry of Regge calculus[26–29] is typically viewed as an approximation to the continuous spacetime manifold of general relativity (GR), it could be that discrete spacetime is fundamental while “the usual continuum theory is very likely only an approximation[25]” and that is what we assume (section II). Further, the links of a Regge calculus graph can connect non-neighboring points of the GR spacetime manifold leading to small corrections to the corresponding GR spacetime geometry. The direct connection between non-neighboring points on the spacetime manifold is referred to as “disordered locality”[30] and has been used on astrophysical scales to explain dark energy[31]. Our views deviate from the standard use of Regge calculus, so we refer to our approach as modified Regge calculus (MORC). We used MORC to generate a fit of the Union2 Compilation supernova data matching that of Λ CDM via a simple perturbative geometric correction of proper distance in Einstein-deSitter (EdS) cosmology[32, 33]. The resulting explanation did not harbor accelerating expansion, so there was no need of a cosmological constant or dark energy. Similarly here, we use MORC without DM to fit galactic RC's rivaling MOND (section III) by assuming disordered locality as well as “contextuality,” i.e., matter can simultaneously have two different values of mass. In this case, the mass of matter interior to the Schwarzschild solution (proper mass) can differ from the mass of that same matter in the surrounding Schwarzschild metric (dynamic mass). We then use this same approach to fit the mass profiles of X-ray clusters rivaling MSTG (section IV). We argue that such modifications are perturbative (small) in the context of the GR spacetime geometry. While we argue that the idea can be extended to dark matter phenomena on cosmological scales, we do not undertake a fit of the CMB angular power spectrum here. Essentially, we claim that large discrepancies observed between proper mass and dynamic mass on galactic and galactic cluster scales in the context of GR spacetime can be understood as resulting from small corrections to the GR spacetime geometry. We therefore conclude (section V) that MORC's contextuality and disordered locality may resolve the dark matter problem on galactic and galactic cluster scales without non-baryonic dark matter, as do MOND and MSTG, respectively. Since the MORC approach to the dark matter problem can be extended

to cosmology and has already been used to explain away dark energy, dark matter and dark energy phenomena may simply reflect geometric perturbations to idealized spacetime structure on large scales.

II. MORC, MOND AND MSTG APPROACHES

Regge calculus is typically viewed as a discrete approximation to GR where the discrete counterpart to Einstein's equations is obtained from the least action principle on a 4D graph. This generates a rule for constructing a discrete approximation to the spacetime manifold of GR using small, contiguous 4D Minkowskian graphical ‘tetrahedra’ called “simplices.” The smaller the legs of the simplices, the better one may approximate a differentiable manifold via a lattice spacetime (Figure 1). Curvature in Regge calculus is represented by “deficit angles” (Figure 2) about any plane orthogonal to a “hinge” (triangular/polygon side of a tetrahedron/3D volume, which is a side of a 4D simplex), so curvature is said to reside on the hinges. A hinge is two dimensions less than the lattice dimension, so in 2D a hinge is a zero-dimensional point (Figure 2). The Hilbert action for a vacuum lattice is (geometrized units)[34]

$$I_R = \frac{1}{8\pi} \sum_{\sigma_i \in L} \varepsilon_i A_i \quad (1)$$

where σ_i is a triangular hinge in the lattice L , A_i is the area of σ_i and ε_i is the deficit angle associated with σ_i . The counterpart to Einstein's equations is then obtained by demanding $\frac{\delta I_R}{\delta \ell_j^2} = 0$ where ℓ_j^2 is the squared length of the j^{th} lattice edge, i.e., the metric. To obtain equations in the presence of matter-energy, one simply adds the matter-energy action I_M to I_R and carries out the variation as before to obtain

$$\frac{\delta I_R}{\delta \ell_j^2} = -\frac{\delta I_M}{\delta \ell_j^2} \quad (2)$$

The LHS of Eq(2) becomes

$$\frac{\delta I_R}{\delta \ell_j^2} = \frac{1}{16\pi} \sum_{\sigma_i \in L} \varepsilon_i \cot \Theta_{ij} \quad (3)$$

where Θ_{ij} is the angle opposite edge ℓ_j in hinge σ_i . One finds the stress-energy tensor is associated with lattice edges, just as the metric, and Regge's equations are to be satisfied for any particular choice of the two tensors on the lattice.

The modification to Regge calculus we propose is to add links between non-neighboring points in the context of the corresponding continuous spacetime manifold, i.e., disordered locality. Then, one would solve Regge's equations for the lattice as before (modified per disordered locality), except that now there is an additional complication in that the LHS of Eq(2) no longer has the simple analytic form given by Eq(3). Indeed, without some highly

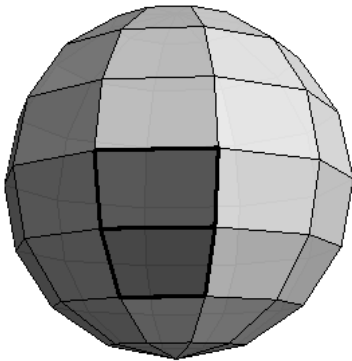


FIG. 1. Regge simplices on the 2-sphere.

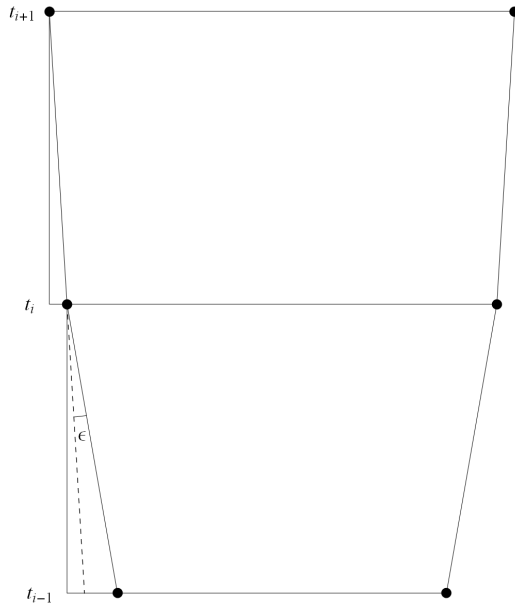


FIG. 2. Deficit angle ϵ for Regge simplices on the 2-sphere.

symmetric form of disordered locality, we would not expect a counterpart to Eq(3) and the modified Regge's equations would have to be solved numerically. Thus, we assume the existence of modest disordered locality in the exact Regge calculus graph justifies small corrections to the corresponding approximate GR solution (which assumes only local interactions per the Hausdorff topology of the GR differentiable manifold). We should note here that an "exact Regge calculus graph" would contain a link for every quantum exchange. Certainly no such solution could ever be generated, so in practice we imagine modified Regge calculus graphs with greatly simplifying assumptions would be used as approximations of the exact Regge calculus graph (also true of standard Regge calculus, obviously). When all link lengths are small,

i.e., in the absence of disordered locality, these approximate Regge calculus solutions would then correspond to GR solutions, i.e., we have standard Regge calculus[35–37]. As with GR solutions, Regge calculus solutions are difficult to obtain and there is no reason to believe that finding extrema of a Regge graphical action modified per disordered locality would be any easier. Rather, at this point, we are simply operating on the assumption that a modified Regge graphical action and its extrema will make correspondence with Regge calculus and GR in the proper limits. Motivated by RBW's prediction of disordered locality with its violation of the Hausdorff nature of GR's spacetime manifold, we are systematically exploring possible geometric corrections to astrophysical phenomena that may be examples of disordered locality. It seems to us that dark energy and dark matter are two such examples. If we can find simple perturbative geometric corrections that resolve the problems of dark energy and dark matter, then we will use these as guides to the construction of a simplified cosmological Regge graphical action modified per disordered locality. In the case of dark energy as pertains to the Union2 Compilation supernova data, we speculated on a perturbative geometric correction to proper distance in EdS cosmology. Here, we explore possible perturbative geometric corrections to resolve the dark matter problem as pertains to galactic RC's and mass profiles of X-ray clusters, and we argue that this approach can be extended to cosmology. Given we do not yet have a graphical action for MORC, it is not as well-developed as MOND and MSTG. Rather, at this stage, the fits we present constitute a feasibility study. We begin with MORC's approach to galactic RC's, which is then easily extended to galactic clusters.

Since galactic RC's are expected to follow Newtonian predictions to the technical limits of current astronomical observations, the metric is simply that of Newtonian spacetime, i.e., we will talk unambiguously about spatial hypersurfaces and consider Newtonian potentials as small perturbations to the background GR spacetime structure. In the case of galactic RC's and galactic clusters, the GR background spacetime is flat. For cosmology, the GR background spacetime is Friedmann-Robertson-Walker (FRW). Our use of GR spacetime with perturbing Newtonian potentials is called the "Newtonian gauge"[38]. Although "The Kerr metric does not represent the exterior metric of a physically likely source, nor the metric during any realistic gravitational collapse"[39], we might nonetheless consider it structurally since rotating galaxies are *prima facie* axisymmetric. In Boyer-Linquist coordinates, the Kerr metric is (geometrized units)

$$ds^2 = - \left(1 - \frac{2Mr}{\Sigma} \right) dt^2 - \frac{4Mars\sin^2\theta}{\Sigma} dt d\phi + \frac{\Sigma}{\Delta} dr^2 + \Sigma d\theta^2 + r^2 \left(1 + \frac{a^2}{r^2} + \frac{2Ma^2\sin^2\theta}{r\Sigma} \right) d\phi^2 \quad (4)$$

where $\Sigma = r^2 + a^2\cos^2\theta$ and $\Delta = r^2 - 2Mr + a^2$. This

reduces to the Schwarzschild metric

$$ds^2 = - \left(1 - \frac{2M}{r}\right) dt^2 + \left(1 - \frac{2M}{r}\right)^{-1} dr^2 + r^2 d\Omega^2 \quad (5)$$

when $a \ll r$ ($a = \frac{J}{M}$ is the angular momentum per unit mass). If for a given galactic orbital radius r we assume all the mass M interior to that radius resides in a radially and axially thin, disk-shaped annulus at r with orbital velocity v in order to generate the most conservative (largest) estimate of J , we have $a = \frac{Mr^2\omega}{Mc} = r\frac{v}{c}$ (restoring c). Since, the largest galactic orbital velocities are about 300 km/s, we have $a \sim r/1000$ so we will use the much simpler Schwarzschild metric for our discussions. Such approximations are not unusual in astrophysics, since it is the case that “for realistic distributions of matter in galaxies, we have neither analytic, nor numerical solutions to general relativity from which orbits can be predicted”[40].

The metric modification we propose has to do with “contextuality,” i.e., matter can have different values of mass in different contexts, e.g., the mass of a free neutron is greater than the mass of a neutron in a nucleus. As regards the mass of baryonic matter in galaxies, the same baryonic matter can have two different values of mass at the same time by virtue of its simultaneous existence in two different contexts. For example, when a Schwarzschild vacuum surrounds a spherical matter distribution the proper mass M_p of the matter (the mass measured locally in the matter) can be different than the dynamical mass M in the Schwarzschild metric responsible for orbital kinematics about the matter[41]. We apply that idea here to each “infinitesimal” annulus of matter in orbit around the galactic center. The mass of that annulus of matter as measured by mass-to-luminosity ratios is its proper mass dM_p while the dynamical mass it contributes to orbiting annuli at larger orbital radii dM differs from dM_p . For example, suppose a Schwarzschild vacuum surrounds a sphere of FRW dust connected at the instantaneously null Schwarzschild radial coordinate. The dynamic mass M of the surrounding Schwarzschild metric is related to the proper mass M_p of the FRW dust by[42]

$$\frac{M_p}{M} = \begin{cases} 1 & \text{flat} \\ \frac{3(\eta - \sin(\eta))}{4\sin^3(\eta/2)} & \geq 1 \quad \text{positively curved} \\ \frac{3(\sinh(\eta) - \eta)}{4\sinh^3(\eta/2)} & \leq 1 \quad \text{negatively curved} \end{cases} \quad (6)$$

That $M = M_p$ for the spatially flat FRW dust (EdS cosmology) follows in part from the fact that the spatial curvature scalar equals zero ${}^{(3)}R = 0$ for the Schwarzschild metric.

Of course, in the GR sense, we’re not local to the stars and gas orbiting the center of a distant galaxy. However,

our measurements of mass-to-luminosity ratios (M/L) are based on local measurements, e.g., objects in close orbits to stars. Thus, when we infer a mass based on M/L, our measurements are de facto local to that matter, so we are measuring dM_p for each annulus via its luminosity even though the galaxy is millions of parsecs away. [This is motivated by RBW’s version of direct particle interaction, which in its original form would require a modification to general relativistic astrophysics in and of itself [43–48].] The MORC graph then has the mass dM_p associated with the links between a given orbiting annulus of matter and Earth while the mass associated with the link(s) connecting the orbital annulus of matter to stellar matter orbiting at larger radii is dM which can differ from dM_p . If, for example, the annulus of orbiting matter had a mass other than dM_p for the links connecting it to Earth, we would see the atomic spectra change accordingly. We do not attribute changes in the atomic spectra of atoms from distant galaxies to such changes in mass, so we tacitly assume that the matter has mass dM_p in the context of its direct interaction with us. Viewed graphically, matter might be thought of as residing on nodes while the mass of that matter would reside on links, as we stated supra concerning the stress-energy tensor in Regge calculus. Different links associated with one and the same node could have different values of mass. The result of this view is that mass is a characterization of spacetime geometry, itself a system of relations, it’s not an intrinsic property of matter.

Accordingly, small differences in spacetime geometry can be characterized by relatively large differences in the values of mass. For example, while M can be $\sim 10M_p$, the deviation from flat spacetime on typical galactic scales per $\frac{2GM(r)}{c^2r}$ is negligible given current technical limits on astronomical observations. Assuming circular orbits (which is common for fitting galactic RC’s) we have $v^2r = GM(r)$, where $M(r)$ is the dynamic mass inside the circular orbit at radius r and v is the orbital speed.

This gives $\frac{2GM(r)}{c^2r} = 2\frac{v^2}{c^2}$. Again, the largest galactic rotation speeds are typically only $10^{-3}c$ so the metric deviation from flat spacetime is $\sim 10^{-6}$ and $M \sim 10M_p$ constitutes an empirically small metric correction.

Another way to quantify the difference geometrically between M and M_p is to use ${}^{(3)}R = \frac{16\pi G\rho}{c^2}$ [49] on galactic scales (where ρ is the mass density). Assuming constant mass density (typical in a galactic bulge) out to radius r where we have orbital velocity v , we have $\frac{16\pi G\rho}{c^2} = \frac{12v^2}{r^2c^2}$. Constant density means $M(r) \sim r^3$ so

$$v(r) = \sqrt{\frac{GM(r)}{r}} \quad (7)$$

increases linearly with distance from zero to its max value v_{max} . Assuming this happens at the radius of the bulge r_b (galactic RC’s actually peak farther out, so this over-

estimates the effect), we have ${}^{(3)}R = \frac{12v_{max}^2}{r_b^2 c^2}$ for the spatial curvature scalar in the annulus at r rather than its Schwarzschild value of zero. $v_{max} \approx 300\text{km/s}$ and $r_b \approx 2000\text{pc}$ gives ${}^{(3)}R \sim 10^{-45}/\text{m}^2$. So, a factor of ten one way or the other in ρ is geometrically inconsequential in this context. Another way to state this, in terms of modified Regge calculus, is that the variation in the deficit angles that accounts for the variation of ρ we're proposing on galactic scales is minuscule. For all these reasons, we believe it's not unreasonable to speculate on a MORC perturbative correction to GR spacetime geometry that changes the mass dM_p in order to fit galactic RC's without non-baryonic dark matter.

In the MOND approach with spherical symmetry and circular orbits, as is commonly used for fitting galactic RC's, it is the Newtonian acceleration

$$a_N(r) = \frac{GM(r)}{r^2} \quad (8)$$

that is modified by the so-called interpolating function $\mu(x)$ where $x = \left| \frac{a(r)}{a_o} \right|$ with a_o a universal constant so that

$$\mu(x)a(r) = \frac{GM(r)}{r^2} \quad (9)$$

$\mu(x) \sim x$ for $x \ll 1$ and $\mu(x) \sim 1$ for $x \gg 1$. Of course, $\mu(x(r))$ means one could view Eq(9) as a modification to $M(r)$ or G as in MSTG [40]

$$a(r) = \frac{GM(r)}{\mu(r)r^2} \quad (10)$$

where $G(r) = \frac{G}{\mu(r)}$ in MSTG. In terms of the Newtonian potential Φ , the Schwarzschild metric is

$$ds^2 = -c^2 \left(1 + \frac{2\Phi}{c^2} \right) dt^2 + \left(1 + \frac{2\Phi}{c^2} \right)^{-1} dr^2 + r^2 d\Omega^2 \quad (11)$$

where $a(r) = |\nabla(\Phi)|$. So, in that sense, MORC, MOND and MSTG can all be viewed as MOG [40]. Therefore, the MORC and MOND fits for THINGS data in section III need not be viewed as evidence for any particular theoretical justification. Applications beyond astrophysics and cosmology will ultimately adjudicate between competing theoretical justifications. Here, we seek only to test MORC's approach to fitting galactic RC's by comparing it to MOND using data where MOND fits were deemed "very successful" [50].

In the MOND fits of section III, we will use the so-called "simple" μ function

$$\mu(x) = \frac{x}{1+x} \quad (12)$$

which Gentile et al. found most successful with the THINGS data[50]. We will also adopt their median best-fit value of the acceleration parameter for the simple μ

function, $a_o = (1.22 \pm 0.33) \times 10^{-8} \text{ cm s}^{-2}$. Generally speaking, MOND has a single fit parameter, M/L for the stellar disk, although when bulge data is available independent of the stellar disk, an additional M/L factor can be introduced for the bulge as well. We will also allow galactic distance d to vary up to one sigma from the nominal value in our MOND fits. Gentile et al. called this "d constrained"[50]. Finally, Gentile et al. also note this data is "not obviously dominated by non-circular motions," so we assume circular orbits to obtain the MOND v as related to the Newtonian v_N [51]

$$v^2 = \frac{v_N^2}{2} + \sqrt{\frac{v_N^4}{4} + v_N^2 a_o r} \quad (13)$$

where

$$v_N^2 = v_{gas}^2 + v_{disk}^2 + v_{bulge}^2 \quad (14)$$

Allowing for variation in M/L for the stellar disk and bulge means

$$v_N^2 = v_{gas}^2 + v_{disk}^2 \gamma_{disk} + v_{bulge}^2 \gamma_{bulge} \quad (15)$$

where γ_{disk} and γ_{bulge} are fit parameters. Assuming the distance d to the galaxy can vary means a further correction in M/L (fitting parameter) for all components, call it γ_{dist} , giving

$$v_N^2 = (v_{gas}^2 + v_{disk}^2 \gamma_{disk} + v_{bulge}^2 \gamma_{bulge}) \gamma_{dist} \quad (16)$$

where $r \rightarrow \gamma_{dist} r$ in Eq(13) as well. Eq(13) is then used to fit THINGS data, i.e., $v(r)$, $v_{gas}(r)$, $v_{bulge}(r)$, and $v_{disk}(r)$, using the fit parameters γ_{disk} , γ_{gas} , and γ_{dist} .

MORC computes the baryonic proper mass $M_{p_i}(r)$ for each component i using Eq(7) with $v_i(r)$ supplied by THINGS. Then $dM_{p_i} = M_{p_i}(r_2) - M_{p_i}(r_1)$ for the proper mass of the i^{th} component in an annulus. A geometric modification is applied to each dM_{p_i} according to its radial location to obtain the corresponding dynamic mass dM_i

$$dM_i = \delta_i \left(\frac{r_2 + r_1}{2} \right)^\xi dM_{p_i} \quad (17)$$

where δ_i is a fitting factor for the i^{th} component and ξ is a fitting parameter that is the same for all components. Ultimately, we expect δ_i and ξ to be determined from the MORC graphical action. Thus, as we stated supra, the fitting procedures needed to resolve the problems of dark energy and dark matter should give us a hint as to the graphical action for MORC cosmology. The dM_i are summed to produce $M_i(r)$, which are then summed to produce $M(r)$ which gives $v(r)$ per Eq(7).

For fitting the mass profiles of X-ray clusters, one assumes a spherically symmetric, isothermal distribution of X-ray emitting gas in hydrostatic equilibrium with the gravitational potential[17]. The gas mass profile as determined by the X-ray luminosity is given by

$$M_p(r) = 4\pi \int_0^r \rho(r') r'^2 dr' \quad (18)$$

where

$$\rho(r) = \rho_o \left(1 + \left(\frac{r}{r_c} \right)^2 \right)^{-1.5\beta}. \quad (19)$$

The constants ρ_o , r_c and β are found from fits of the surface density map $\Sigma(x, y)$. $M_p(r)$ corresponds to the “proper mass” for galactic RC’s above. The dynamic mass profile needed for hydrostatic equilibrium at temperature T is given by

$$M(r) = \frac{3\beta kT}{G\mu_A m_p} \left(\frac{r^3}{r^2 + r_c^2} \right) \quad (20)$$

where μ_A is the mean atomic weight of the gas constituents (≈ 0.609), m_p is the mass of the proton, k is the Boltzmann constant, and G is the gravitational constant. In the MSGT version of MOG per Moffat and Brownstein, as stated above, $G \rightarrow G(r)$ and is understood to reduce $M(r)$ of Eq(20) to $M_p(r)$ of Eq(18). Effectively, we have

$$M_p(r) = M(r) + M_o \eta(r) - \sqrt{(M_o \eta(r))^2 + 2M_o M(r) \eta(r)} \quad (21)$$

where

$$\eta(r) = 0.5 \left(1 - \exp(-r/r_o) \left(1 + \frac{r}{r_o} \right)^2 \right) \quad (22)$$

with M_o and r_o fitting parameters and $M(r)$ computed using G in Eq(20). Since we’re assuming spherical symmetry, the MORC approach used for galactic RC’s can be easily adopted here. Contrary to MSTG, in MORC we are increasing $dM_p(r)$ by a geometric factor to give the dynamic mass $M(r)$. Thus, we modify Eq(18) to give

$$M(r) = \int_0^r \delta r^\xi dM_p = 4\pi \int_0^r \delta r'^\xi \rho(r') r'^2 dr' \quad (23)$$

with $\rho(r)$ given by Eq(19) and δ and ξ fitting parameters in analogy to the MORC fits of galactic RC’s. This value of $M(r)$ is then compared to that of Eq(20).

III. MORC AND MOND FITS OF GALACTIC RC’S

We are now ready to compare MORC fits with MOND fits of twelve high-resolution galactic RC’s from The HI Nearby Galaxy Survey[52] used by Gentile et al.[50] to explore MOND fits. Gentile et al. describe these data as “the most reliable for mass modelling, and they are the highest quality RC’s currently available for a sample of galaxies spanning a wide range of luminosities.” Keep in mind that MOND fits are more rigorously constrained, since MOND is a highly developed theory. MORC fits on the other hand are being done to determine feasibility and guidance in constructing a graphical action

Name	δ_{bulge}	δ_{disk}	δ_{gas}	ξ	MSE
NGC 2841	1.23	1.29	10.88	0.25	85.6
	1.33	0.81	4.61	0.50	87.3
	0.96	2.03	25.0	0.00	87.1
	1.27	0.31	0.78	1.00	101
NGC 7331	1.17	0.22	0.00	0.90	17.8
	1.27	0.17	0.00	1.00	22.8
	0.92	0.44	0.71	0.50	31.0
	0.20	0.99	5.50	0.00	52.2
NGC 3521	N/A	0.63	0.95	0.41	125
	N/A	0.87	5.76	0.00	240
	N/A	0.27	0.00	1.00	483
NGC 6946	1.29	0.60	1.13	0.46	30.4
	0.51	0.99	7.52	0.00	40.2
	2.51	0.25	0.00	1.00	60.0
NGC 2903	0.02	1.71	1.02	0.89	95.4
	0.05	1.51	0.73	1.00	97.3
	0.00	2.56	3.36	0.50	123
	0.00	3.76	14.7	0.00	251
NGC 5055	0.47	0.31	1.90	0.53	80.0
	0.27	0.67	10.6	0.00	88.5
	0.63	0.14	0.33	1.00	88.0
NGC 3198	0.033	3.25	35.8	-0.60	8.9
	0.00	3.57	48.2	-0.70	9.2
	0.36	1.52	5.76	0.00	30.9
	0.68	0.70	1.19	0.50	49.9
	0.93	0.30	0.24	1.00	63.4
NGC 3621	N/A	0.96	1.72	0.44	47.4
	N/A	1.24	6.25	0.00	56.0
	N/A	0.54	0.30	1.00	80.3
NGC 2403	N/A	2.28	28.7	-0.50	12.1
	N/A	2.20	34.8	-0.60	16.1
	N/A	2.30	10.1	0.00	44.8
	N/A	1.92	3.00	0.50	130
	N/A	1.42	0.61	1.00	248
NGC 7793	N/A	1.93	4.41	0.30	21.8
	N/A	1.91	2.85	0.50	24.3
	N/A	1.84	8.29	0.00	27.8
	N/A	1.65	0.80	1.00	52.0
NGC 2976	N/A	0.92	4.90	0.00	23.0
	N/A	1.16	0.00	-0.10	23.2
	N/A	1.16	0.00	0.50	36.2
	N/A	1.09	0.00	1.00	77.2
DDO 154	N/A	12.0	3.94	0.22	2.20
	N/A	15.5	2.53	0.50	2.53
	N/A	8.06	5.43	0.00	2.43
	N/A	17.84	1.10	1.00	4.70

TABLE I. MORC fits for THINGS. MSE is in $(\text{km/s})^2$. Corresponding plots are in Figures 4 & 5.

for MORC cosmology. This is akin to allowing the acceleration parameter a_o to vary in MOND fits so as to determine its value as a universal constant. MORC results are in Table I and MOND results are in Table II. Graphical display of the best fits reported below are in Figures 4 & 5. What we note concerning ξ is its broad range, $-0.60 \leq \xi \leq 0.90$. We will find that this range is greatly reduced for X-ray clusters. We used a simple mean square error (MSE or mean χ^2) to quantify the fits.

Name	γ_{bulge}^*	γ_{disk}	γ_{dist}	MSE
NGC 2841	0.99 (1.02)	0.79 (0.70)	1.46 (1.53)	19.5
d constrained	1.09 (1.24)	1.32 (1.20)	1.11 (1.11)	54.1
NGC 7331	1.09 (1.16)	0.98 (0.91)	0.68 (0.71)	18.8
d constrained	1.17 (1.22)	0.59 (0.57)	0.913 (0.913)	28.6
NGC 3521	N/A	1.77 (1.08)	0.44 (0.65)	210
d constrained	N/A	0.93 (0.97)	0.70 (0.70)	264
NGC 6946	0.58 (0.55)	0.94 (0.58)	0.80 (1.09)	29.2
comparison**	0.49 (0.55)	0.59 (0.58)	1.09 (1.09)	32.3
NGC 2903	0.00 (0.00)	2.06 (2.80)	1.25 (1.07)	202
NGC 5055	0.40 (0.47)	0.80 (0.84)	0.66 (0.62)	26.7
d constrained	0.38 (0.43)	0.72 (0.70)	0.70 (0.70)	27.2
NGC 3198***	0.37 (N/A)	1.59 (N/A)	0.58 (0.62)	18.8
d constrained	0.26 (N/A)	0.65 (N/A)	0.89 (0.89)	74.2
NGC 3621	N/A	0.76 (0.75)	0.91 (0.92)	9.14
NGC 2403	N/A	0.69 (0.63)	1.53 (1.46)	34.4
d constrained	N/A	1.29 (1.10)	1.08 (1.08)	42.3
NGC 7793	N/A	0.51 (0.39)	1.52 (1.68)	42.1
d constrained	N/A	1.00 (0.90)	1.10 (1.10)	55.0
NGC 2976	N/A	0.11 (0.09)	2.02 (2.17)	7.83
d constrained	N/A	0.38 (0.36)	1.10 (1.10)	12.0
DDO 154	N/A	4.01 (2.47)	0.64 (0.71)	1.63
d constrained	N/A	1.36 (1.56)	0.75 (0.75)	4.60

TABLE II. MOND fits for THINGS. MSE is in $(\text{km/s})^2$. Values in parentheses are from Gentile et al.[50] fits minimizing reduced χ^2 . If there is no “ d constrained,” the “ d free” fit satisfies “ d constrained.” Corresponding plots are in Figures 4 & 5. *N/A means Gentile et al. did not use independent bulge data. **For comparison with Gentile et al. we fixed $\gamma_{dist} = 1.09$. ***Gentile et al. used composite disk and bulge data in THINGS, while we used the separate disk and bulge data also supplied in THINGS.

IV. MORC AND MSTG FITS OF X-RAY CLUSTERS

Here we will compare MORC to MSTG for fitting the mass profiles of the eleven X-ray clusters found in Brownstein[40] as obtained from Reiprich and Böhringer[53, 54] using combined ROSAT and ASCA data. All data were taken from Brownstein, as well as the parameters for the MSTG best fits, since therein Brownstein found MSTG fits of these X-ray clusters exceeded those of MOND and STVG. As with our comparison of MORC to MOND for galactic RC’s, one should keep in mind that MSTG, as a well-developed theory, is more constrained than MORC, so the comparison between MORC and MSTG here is only for establishing the feasibility of the MORC approach. In each case, we computed proper (or “gas”) mass $M_p(r)$ and dynamic mass $M(r)$ at eleven logarithmically evenly spaced points from 13 kpc to r_{out} , “the point where the density of the X-ray cluster drops to $\approx 10^{-28} \text{ g/cm}^3$ which is about 250 times the mean cosmological density of baryons.” The values of T , ρ_o , β , and r_c , supplied by Brownstein, were used with Eqs(18-20) to compute $M_p(r)$ and $M(r)$. We then computed the MSTG best fit values for $M_p(r)$ at these eleven locations using M_o and r_o , supplied by Brown-

Name	δ	ξ	MSE
Bullet	15.9	-0.092	0.00065
Abell 2142	90.6	-0.36	0.00369
Coma	53.1	-0.22	0.00363
Abell 2255	23.0	-0.088	0.00088
Perseus	176	-0.51	0.00167
Norma	95.3	-0.31	0.00761
Hydra-A	158	-0.47	0.00086
Centaurus	663	-0.65	0.00075
Abell 400	152	-0.41	0.00594
Fornax	87.7	-0.12	0.00041
Messier 49	940	-0.46	0.00029

TABLE III. MORC fits for mass profiles of X-ray clusters. MSE is $(\Delta \text{Log}(M))^2$. Corresponding plots are in Figures 6 & 7.

Name	M_o ($10^{14} M_\odot$)	r_o (kpc)	MSE
Bullet	56.7	116.8	0.0443
Abell 2142	30.0	56.8	0.0302
Coma	30.7	88.2	0.0342
Abell 2255	43.8	157.4	0.0386
Perseus	10.7	23.5	0.0239
Norma	30.1	97.6	0.0373
Hydra-A	9.5	23.9	0.0348
Centaurus	10.0	14.2	0.0218
Abell 400	6.0	44.7	0.0124
Fornax	13.7	67.4	0.0318
Messier 49	10.3	10.8	0.0244

TABLE IV. MSTG fits for mass profiles of X-ray clusters. M_o and r_o were taken from Brownstein [40]. MSE is $(\Delta \text{Log}(M))^2$. Corresponding plots are in Figures 6 & 7.

stein, with Eqs(21 & 22). MORC’s best values of δ and ξ were found for fitting the dynamic mass $M(r)$ of Eq(23). As with galactic RC’s, we computed a simple MSE to quantify the fits (MSE is logarithmic, since we did a log-log plot of the fits). The plots of these best fits are in Figures 6 & 7. MORC results are in Table III and MSTG results are in Table IV. Overall, we find the MORC fits to be comparable to those of MSTG.

What we note concerning ξ is its range, $-0.65 \leq \xi \leq -0.088$, in comparison to galactic RC’s. Here the range of ξ is about half that found for galactic RC’s and is strictly negative. An explanation will have to wait until we finish MORC fits of cosmological data. At that point we will have MORC fits for dark energy and dark matter phenomena to include supernovae data, galactic RC’s, mass profiles for X-ray galaxy clusters, and the angular power spectrum of the CMB. With all these fits in hand, we will look for clues hinting at a possible MORC cosmology model with disordered locality, which should explain the fitting parameters.

Regarding cosmology, the Newtonian potential disappears from GR’s FRW models with their homogeneity and isotropy, so the average value of MSTG’s skew sym-

metric field is zero[55, 56]. In this case, the gravitational constant of MSTG runs in time, i.e., $G \rightarrow G(t)$ instead of $G \rightarrow G(r)$. Conversely, the graphical form of Regge calculus cosmology maintains a Newtonian potential in its simplices. As we showed[32], the Regge equation for EdS cosmology with continuous time is

$$\frac{\pi - \cos^{-1} \left(\frac{v^2/c^2}{2(v^2/c^2+2)} \right) - 2 \cos^{-1} \left(\frac{\sqrt{3v^2/c^2+4}}{2\sqrt{v^2/c^2+2}} \right)}{\sqrt{v^2/c^2 + 4}} = \frac{Gm}{2rc^2} \quad (24)$$

With $v^2/c^2 \ll 1$ an expansion of the LHS of Eq(24) gives

$$\frac{v^2}{4c^2} + \mathcal{O} \left(\frac{v}{c} \right)^4 = \frac{Gm}{2rc^2} \quad (25)$$

Thus, to leading order (defining “small” simplices) we have $\frac{v^2}{2} = \frac{Gm}{r}$, which is just a Newtonian conservation of energy expression for a unit mass moving at escape velocity v at distance r from mass m . Here, m is the dynamic mass, which exceeds the proper mass obtained via M/L ratios, just like our analyses above. There is no MORC “fit” of this mass difference in this uniform global context, given the mass difference between baryonic mass and the dynamic mass needed to provide a spatially flat model currently supported by Planck data[57] is a universal scalar. However, this universal scalar should be explained by a MORC graphical action for cosmology.

What we rather need to do at this time is fit the CMB angular power spectrum, since DM is assumed to play an important role in the formation of anisotropies therein[58]. That is because anisotropies in the CMB angular power spectrum are understood to arise in part from spatial inhomogeneities in the matter distribution during the radiation dominated era. Accordingly, the spatially flat FRW metric (geometrized units)[38]

$$ds^2 = -dt^2 + a^2(t)\delta_{ij}dx^i dx^j \quad (26)$$

is modified in the conformal Newtonian gauge to read

$$ds^2 = -(1 + 2\Phi)dt^2 + (1 + 2\Psi)a^2(t)\delta_{ij}dx^i dx^j \quad (27)$$

where Φ can be interpreted as the Newtonian potential and Ψ is a perturbation to the spatial curvature. When pressure is negligible, $\Psi = -\Phi$. Since the spatial part of the Schwarzschild metric can be written[49]

$$ds^2 = \left(1 + \frac{M}{2r}\right)^4 \delta_{ij}dx^i dx^j \quad (28)$$

we have for small $\frac{M}{2r} \left(= -\frac{\Phi}{2}\right)$

$$ds^2 \approx \left(1 + \frac{2M}{r}\right) \delta_{ij}dx^i dx^j \quad (29)$$

which explains the perturbation in Eq(27) as a small Newtonian potential in Eq(11) placed in a spatially flat

FRW background. Thus, our MORC approach should be amenable to explaining anisotropies in the CMB angular power spectrum without DM.

Finally, we point out that gravitational lensing data of the Bullet Cluster (1E0657-558) originally touted as “direct empirical proof of the existence of dark matter”[59], can be explained without DM[60]. What happened in this case is a small galactic cluster (“subcluster”) collided with the larger Bullet Cluster. The galaxies of both clusters passed through the collision region relatively unaffected, but the intracluster medium (ICM) gas of the two clusters was left behind in the collision region. The result was four lobes of baryonic matter aligned as follows: the galaxies of the Bullet Cluster, the gas of the Bullet Cluster, the gas of the subcluster, and the galaxies of the subcluster (Figure 3). If one accepts that the mass of the cluster galaxies is only 10% of the baryonic mass, then in the absence of DM one would expect gravitational lensing maps of this region (blue lobes in Figure 3) to overlap X-ray images of the gas lobes (red lobes in Figure 3), since the gas possesses 90% of the baryonic mass. What Clowe et al. rather found[59] was that the lensing peaks were located in the galaxy lobes, so the galaxies are inside the blue lobes of Figure 3. Their conclusion was that there exists large quantities of DM which passed through the collision with the galaxies. Brownstein and Moffat[60] explained the offset lensing peaks using MSTG because $G(r)$ associated with the galaxies increases more than $G(r)$ associated with the gas, since the galaxies are farther removed from the center of the Newtonian gravitational potential. The explanation in MORC would be similar, since G is associated with ρ in Einstein’s equations, i.e., the proper mass of each of the galaxy and gas lobes is increased to a larger dynamic mass. Since the galaxies are farther removed from the center of the Newtonian gravitational potential, the dynamic mass of the galaxies exceeds the dynamic mass of the gas leading to lensing peaks in the galaxy lobes. A MORC fit of the offset at this point is of no interest, since the number of fitting parameters would equal the number of data points. Again, once the fitting parameters are specified by the MORC cosmology model, we will return to fit this offset lensing data.

V. CONCLUSION

We used modified Regge calculus (MORC) to argue that the mass of baryonic matter on astronomical scales can simultaneously have two different values (contextuality), i.e., the proper mass measured per mass-to-luminosity ratios (disordered locality) and the dynamical mass measured per orbital mechanics associated with the Newtonian gravitational potential. We showed that a difference between proper mass and dynamical mass as large as a factor of ten is geometrically insignificant, so our proposed corresponding MORC geometric modifications are “small.” Essentially, we claim that large discrepan-

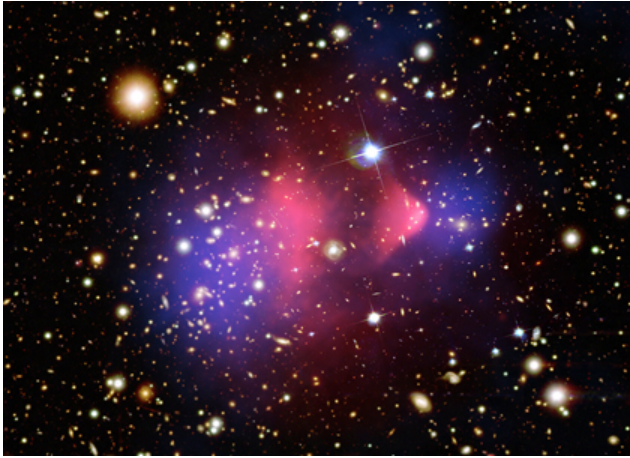


FIG. 3. Bullet Cluster X-ray and lensing composite (false color) image from NASA Release 06-297. Blue lobes are lensing data in vicinity of the galaxies. Red lobes are X-ray images of ICM gas left behind after the subcluster (right side) passed through the Bullet Cluster (left side).

cies observed between proper mass and dynamic mass on galactic and galactic cluster scales in the context of GR spacetime can be understood as resulting from perturbative corrections to the GR spacetime geometry, since mass is a characterization of spacetime geometry not an intrinsic property of matter. Thus, we explored a possible perturbative geometric modification to the proper mass that would resolve the dark matter problem on galactic scales by fitting “the highest quality RC’s currently available for a sample of galaxies spanning a wide range of luminosities”[50]. We found MORC fits were comparable

to MOND fits, which were already deemed “very successful”[50] for these data. We then showed that a similar geometric modification to the proper mass of X-ray clusters would account for their much larger dynamic mass by fitting the mass profiles of eleven X-ray clusters found in Brownstein[40] as obtained from Reiprich and Böhringer[53, 54]. The resulting MORC fits were comparable to those of MSTG, which also does not require non-baryonic dark matter and was found to provide superior fits to both MOND and STVG for the same data[17, 40]. We therefore conclude that MORC’s contextuality and disordered locality may resolve the dark matter problem on galactic and galactic cluster scales without non-baryonic dark matter. Since the MORC approach to the dark matter problem can be extended to cosmology and has already been used to explain away dark energy as pertains to supernova data[32, 33], dark matter and dark energy phenomena may simply reflect geometric perturbations to idealized spacetime structure on large scales. We will next bring MORC to bear on fitting the CMB angular power spectrum. All such MORC solutions would then provide a guide to the construct of a graphical action with disordered locality for MORC cosmology.

ACKNOWLEDGEMENTS

We thank Erwin de Blok for providing the THINGS data, Gianfranco Gentile for providing information about his MOND fits, and Joel Brownstein for providing information about MSTG.

REFERENCES

- [1] Oort, J.H.: The force exerted by the stellar system in the direction perpendicular to the galactic plane and some related problems. *Bulletin of the Astronomical Institutes of the Netherlands* 151, 249 (1932).
- [2] Zwicky, F.: Spectral displacement of extra galactic nebulae. *Helvetica Physica Acta* 6, 110-127 (1933).
- [3] Zwicky, F.: On the masses of nebulae and clusters of nebulae. *The Astrophysical Journal* 86, 217-246 (1937).
- [4] Rubin, V., and Ford, K: Rotation of the Andromeda nebula from a spectroscopic survey of emission regions. *The Astrophysical Journal* 159, 379-403 (1970).
- [5] Garrett, K., and Duda, G.: Dark Matter: A Primer. *Advances in Astronomy* 2011, doi:10.1155/2011/968283 (2011).
- [6] Munoz, C.: Dark matter detection in the light of recent experimental results. *International Journal of Modern Physics A* 19, 3093-3170 (2004).
- [7] Feng, J.: Dark Matter Candidates from Particle Physics and Methods of Detection. *Annual Reviews of Astronomy and Astrophysics* 48, 495 (2010) <http://arxiv.org/abs/1003.0904>
- [8] Milgrom, M.: A modification of the Newtonian dynamics as a possible alternative to the hidden mass hypothesis. *The Astrophysical Journal* 270, 365-370 (1983).
- [9] Milgrom, M: MOND theory. *Canadian Journal of Physics* 93, 107 (2015) <http://arxiv.org/abs/1404.7661>
- [10] Sanders, R.H., and McGaugh, S.: Modified Newtonian Dynamics as an Alternative to Dark Matter. *Annual Reviews of Astronomy & Astrophysics* 40, 263-317 (2002) <http://arxiv.org/abs/astro-ph/0204521>
- [11] Bekenstein, J.D.: Relativistic gravitation theory for the modified Newtonian dynamics paradigm. *Physical Review D* 70, 083509 (2004).
- [12] Sanders, R.H.: A tensor-vector-scalar framework for modified dynamics and cosmic dark matter. *Monthly Notices of the Royal Astronomical Society* 363, 459 (2005).
- [13] Zlosnik, T., Ferreira, P., and Starkman, G.: Modifying gravity with the aether: An alternative to dark matter. *Physical Review D* 75, 044017 (2007) <http://arxiv.org/abs/astro-ph/0607411>
- [14] Zhao, H.S., and Li, B.: Dark Fluid: A Unified framework for Modified Newtonian Dynamics, Dark Matter, and Dark Energy. *The Astrophysical Journal* 712,

doi:10.1088/0004-637X/712/1/130 (2010).

[15] Blanchet, L., and Le Tiec, A.: Model of dark matter and dark energy based on gravitational polarization. *Physical Review D* 78, 024031 (2008).

[16] Brownstein, J.R., and Moffat, J.W.: Galaxy Rotation Curves Without Non-Baryonic Dark Matter. *The Astrophysical Journal* 636, 721-741 (2006).

[17] Brownstein, J.R., and Moffat, J.W.: Galaxy Cluster Masses Without Non-Baryonic Dark Matter. *Monthly Notices of the Royal Astronomical Society* 367, 527-540 (2006) <http://arxiv.org/abs/astro-ph/0507222>

[18] Bergstrom, L.: Non-baryonic dark matter: observational evidence and detection methods. *2000 Reports on Progress in Physics* 63, 793 doi:10.1088/0034-4885/63/5/2r3

[19] Gentile, G., Burkert, A., Salucci, P., Klein, U., and Walter, F.: The Dwarf Galaxy DDO 47 as a Dark Matter Laboratory: Testing Cusps Hiding in Triaxial Halos. *The Astrophysical Journal Letters* 634, doi:10.1086/498939 (2005) <http://arxiv.org/pdf/astro-ph/0506538.pdf>

[20] Stuckey, W.M., Silberstein, M., and McDevitt, T.: Relational Blockworld: Providing a Realist Psi-Epistemic Account of Quantum Mechanics. *International Journal of Quantum Foundations* 1, 123-170 (2015) <http://www.ijqf.org/wps/wp-content/uploads/2015/06/IJQF2015v1n3p2.pdf>

[21] Stuckey, W.M., Silberstein, M., and Cifone, M.: Reconciling spacetime and the quantum: Relational Blockworld and the quantum liar paradox. *Foundations of Physics* 38, 348-383 (2008) <http://arxiv.org/abs/quant-ph/051009>

[22] Silberstein, M., Stuckey, W.M., and Cifone, M.: Why quantum mechanics favors adynamical and acausal interpretations such as Relational Blockworld over backwardly causal and time-symmetric rivals. *Studies in History & Philosophy of Modern Physics* 39(4), 736-751 (2008)

[23] Silberstein, M., Stuckey, W.M., and McDevitt, T.: Being, Becoming and the Undivided Universe: A Dialogue between Relational Blockworld and the Implicate Order Concerning the Unification of Relativity and Quantum Theory. *Foundations of Physics* 43, 502-532 (2013) <http://arxiv.org/abs/1108.2261>

[24] Stuckey, W.M., Silberstein, M., and McDevitt, T.: An Adynamical, Graphical Approach to Quantum Gravity and Unification: Forthcoming In: Licata, I (ed.) *The Algebraic Way: Space, Time and Quantum Beyond Peaceful Coexistence*, Imperial College Press, London (2015) <http://arxiv.org/abs/0908.4348>

[25] Feinberg, G., Friedberg, R., Lee, T.D., Ren, H.C.: Lattice Gravity Near the Continuum Limit. *Nuclear Physics B* 245, 343-368 (1984)

[26] Regge, T.: General relativity without coordinates. *Nuovo Cimento* 19, 558571 (1961)

[27] Misner, C.W., Thorne, K.S., Wheeler, J.A.: *Gravitation*. W.H. Freeman, San Francisco (1973), Chapter 42, p 1166.

[28] Barrett, J.W.: The geometry of classical Regge calculus. *Classical and Quantum Gravity* 4, 15651576 (1987)

[29] Williams, R.M., Tuckey, P.A.: Regge calculus: a brief review and bibliography. *Classical and Quantum Gravity* 9, 14091422 (1992)

[30] Caravelli, F., and Markopoulou, F.: Disordered Locality and Lorentz Dispersion Relations: An Explicit Model of Quantum Foam (2012) <http://arxiv.org/pdf/1201.3206v1.pdf>

[31] Prescod-Weinstein, C., and Smolin, L.: Disordered Locality as an Explanation for the Dark Energy. *Physical Review D* 80, 063505 (2009) <http://arxiv.org/pdf/0903.5303.pdf>

[32] Stuckey, W.M., McDevitt, T., and Silberstein, M.: Modified Regge Calculus as an Explanation of Dark Energy. *Classical and Quantum Gravity* 29, 055015 (2012a) <http://arxiv.org/abs/1110.3973>

[33] Stuckey, W.M., McDevitt, T., and Silberstein, M.: Explaining the Supernova Data without Accelerating Expansion. *International Journal of Modern Physics D* 21(11), 1242021 (2012b).

[34] Sorkin, R.: The electromagnetic field on a simplicial net. *Journal of Mathematical Physics* 16, 2432-2440 (1975).

[35] Brewin, L: Is the Regge calculus a consistent approximation to general relativity? *General Relativity & Gravitation* 32, 897-918 (2000).

[36] Miller, M.A.: Regge calculus as a fourth-order method in numerical relativity. *Classical and Quantum Gravity* 12, 3037-3051 (1995).

[37] Brewin, L. and Gentle, A.P.: On the convergence of Regge calculus to general relativity. *Classical and Quantum Gravity* 18, 517-526 (2001).

[38] Hu, W.: Wandering in the Background: A Cosmic Microwave Background Explorer. *PhD Thesis* (1995) <http://arxiv.org/abs/astro-ph/9508126>

[39] Teukolsky, S.: The Kerr Metric. *Classical & Quantum Gravity* 32, 124006 (2015).

[40] Brownstein, J.R.: Modified Gravity and the phantom of dark matter. *PhD Thesis* (2009) <http://arxiv.org/abs/0908.0040>

[41] Wald, R.: *General Relativity*. University of Chicago Press, Chicago (1984), p 126.

[42] Stuckey, W.M.: The observable universe inside a black hole. *American Journal of Physics* 62, 788-795 (1994).

[43] Wheeler, J.A., Feynman, R.P.: Classical Electrodynamics in Terms of Direct Interparticle Action. *Reviews of Modern Physics* 21, 425433 (1949)

[44] Hawking, S.W.: On the Hoyle-Narlikar theory of gravitation. *Proceedings of the Royal Society of London. Series A, Mathematical and Physical Sciences* 286, 313 (1965)

[45] Davies, P.C.W.: Extension of Wheeler-Feynman quantum theory to the relativistic domain I. Scattering processes. *Journal of Physics A: General Physics* 4, 836-845 (1971)

[46] Davies, P.C.W.: Extension of Wheeler-Feynman quantum theory to the relativistic domain II. Emission processes. *Journal of Physics A: General Physics* 5, 1025-1036 (1972)

[47] Hoyle, F., Narlikar, J.V.: Cosmology and action-at-a-distance electrodynamics. *Reviews of Modern Physics* 67, 113-155 (1995)

[48] Narlikar, J.V.: Action at a Distance and Cosmology: A Historical Perspective. *Annual Review of Astronomy and Astrophysics* 41, 169-189.

[49] Wong, C.: Applications of Regge calculus to the Schwarzschild and Reissner-Nordstrom geometries at the moment of time symmetry. *Journal of Mathematical Physics* 12, 70-78 (1971).

[50] Gentile, G., Famaey, B., and de Blok, W.: THINGS about MOND. *Astronomy and Astrophysics A* 76, 527 (2011) <http://arxiv.org/abs/0810.2125v1>

- [51] Richtler, T., Schuberth, Y., Hilker, M., Dirsch, B., Bassino, L., and Romanowsky, A.: The dark matter halo of NGC 1399- CDM or MOND? *Astronomy and Astrophysics* 478, L23-L26. doi:10.1051/0004-6361:20078539 (2008).
- [52] Walter, F., Brinks, E., de Blok, W., Bigiel, F., Kennicutt, R., Thornley, M., and Leroy, A.: THINGS: The HI Nearby Galaxy Survey. *The Astronomical Journal* 136, doi:10.1088/0004-6256/136/6/2563 (2008) <http://arxiv.org/pdf/0810.2125.pdf>
- [53] Reiprich, T.H.: Cosmological Implications and Physical Properties of an X-Ray Flux-Limited Sample of Galaxy Clusters, PhD Thesis (2001)
- [54] Reiprich, T.H., and Böhringer, H.: The Mass Function of an X-Ray Flux-limited Sample of Galaxy Clusters. *The Astrophysical Journal* 567, 716 (2002)
- [55] Moffat, J.W.: Gravitational Theory, Galaxy Rotation Curves and Cosmology without Dark Matter. *Journal of Cosmology and Astroparticle Physics* 2005, <http://dx.doi.org/10.1088/1475-7516/2005/05/003> (2005)
- [56] Moffat, J.W.: A Modified Gravity and its Consequences for the Solar System, *Astrophysics and Cosmology. International Journal of Modern Physics D* 16, 2075-2090 (2008) <http://arxiv.org/abs/gr-qc/0608074>
- [57] Planck Collaboration: Planck 2013 results. XVI. Cosmological parameters. *Astronomy & Astrophysics* 571, DOI: 10.1051/0004-6361/201321591 (2014) <http://arxiv.org/abs/1303.5076>
- [58] Hu, W.: Structure Formation with Generalized Dark Matter. *The Astrophysical Journal* 506, 485-494 (1998) <http://background.uchicago.edu/~whu/Papers/gdm.pdf>
- [59] Clowe, D., Bradac, M., Gonzalez, A., Markevitch, M., Randall, S., Jones, C., and Zaritsky, D.: A Direct Empirical Proof of the Existence of Dark Matter. *The Astrophysical Journal Letters* 648, L109-L113 (2006) <http://arxiv.org/abs/astro-ph/0608407>
- [60] Brownstein, J.R., and Moffat, J.W.: The Bullet Cluster 1E0657-558 evidence shows Modied Gravity in the absence of Dark Matter, *Monthly Notices of the Royal Astronomical Society* 382, 29-47 (2007) arXiv:astro-ph/0702146

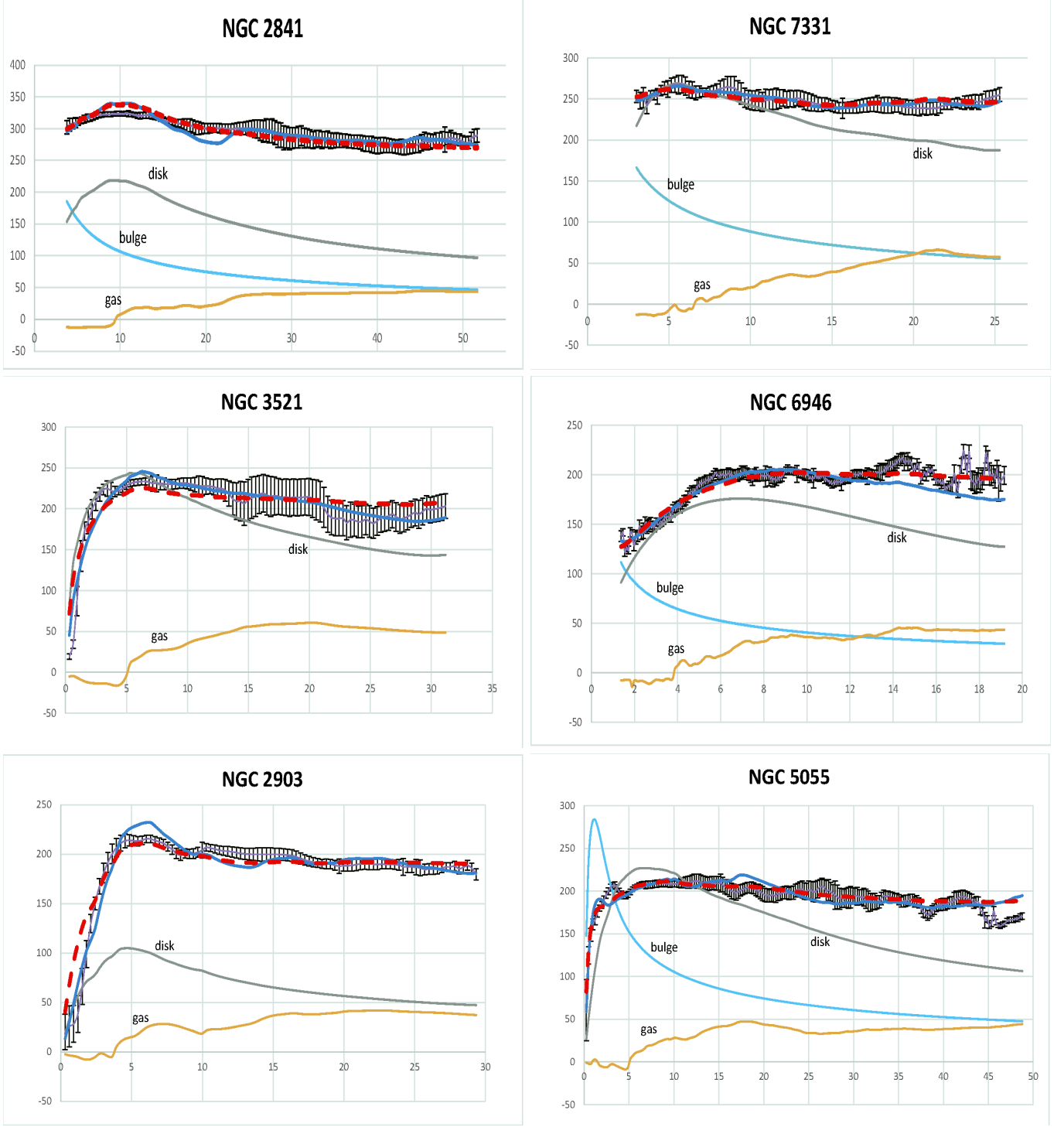


FIG. 4. Graphs of MORC (solid) and MOND (dashed) fits of THINGS galactic RC's (with error bars). MORC disappears when it lies right underneath MOND. Disk, gas and bulge curves are labeled. Bulge curves are not always available. Vertical axis is rotation velocity in km/s and horizontal axis is orbital radius in kpc. Note: The MOND distance fitting factor γ_{dist} would alter the horizontal scale proportionally. Corresponding numerical results are in Tables I & II.

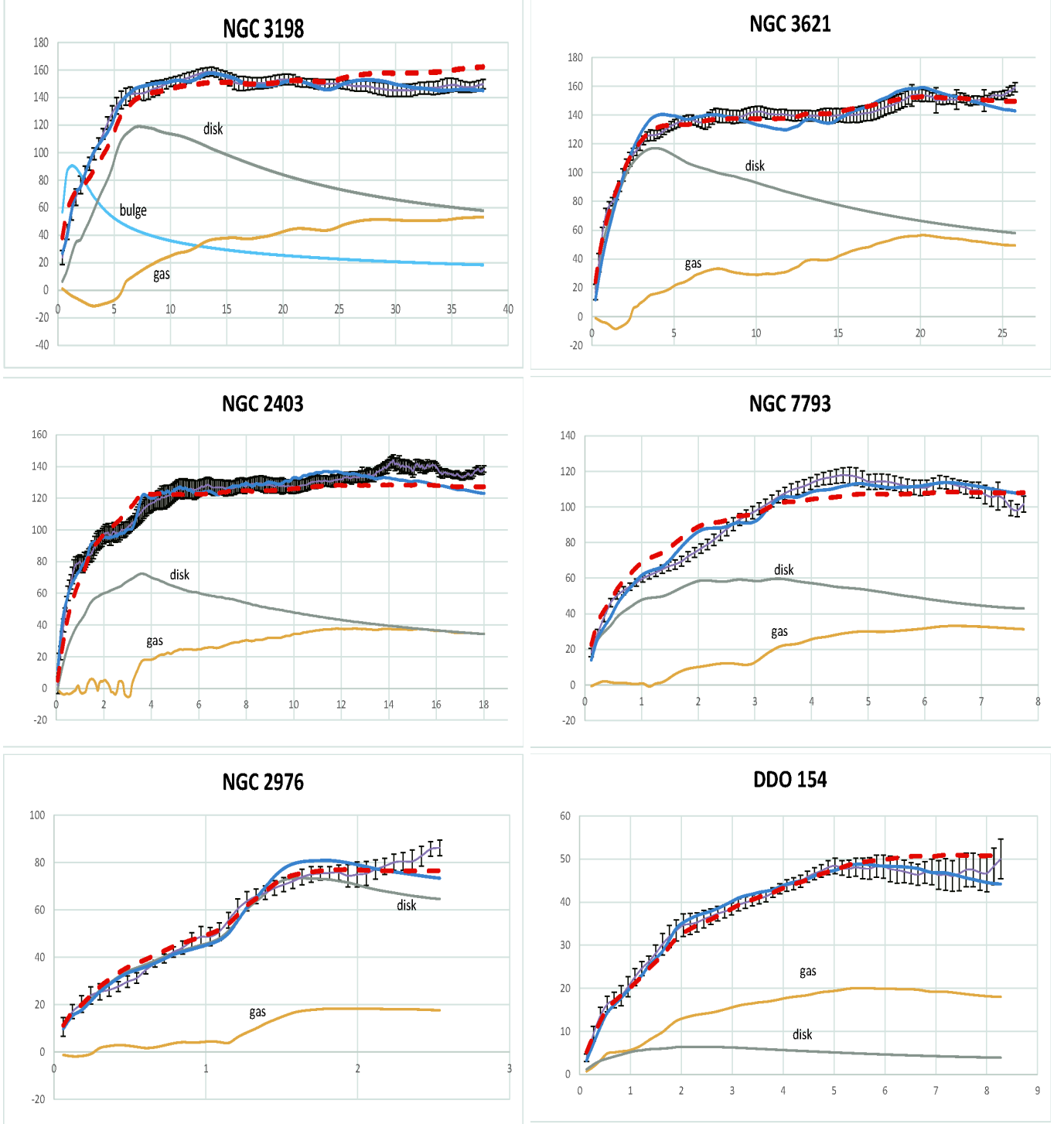


FIG. 5. More graphs of MORC (solid) and MOND (dashed) fits of THINGS galactic RC's (with error bars). MORC disappears when it lies right underneath MOND. Disk, gas and bulge curves are labeled. Bulge curves are not always available. Vertical axis is rotation velocity in km/s and horizontal axis is orbital radius in kpc. Note: The MOND distance fitting factor γ_{dist} would alter the horizontal scale proportionally. Corresponding numerical results are in Tables I & II.

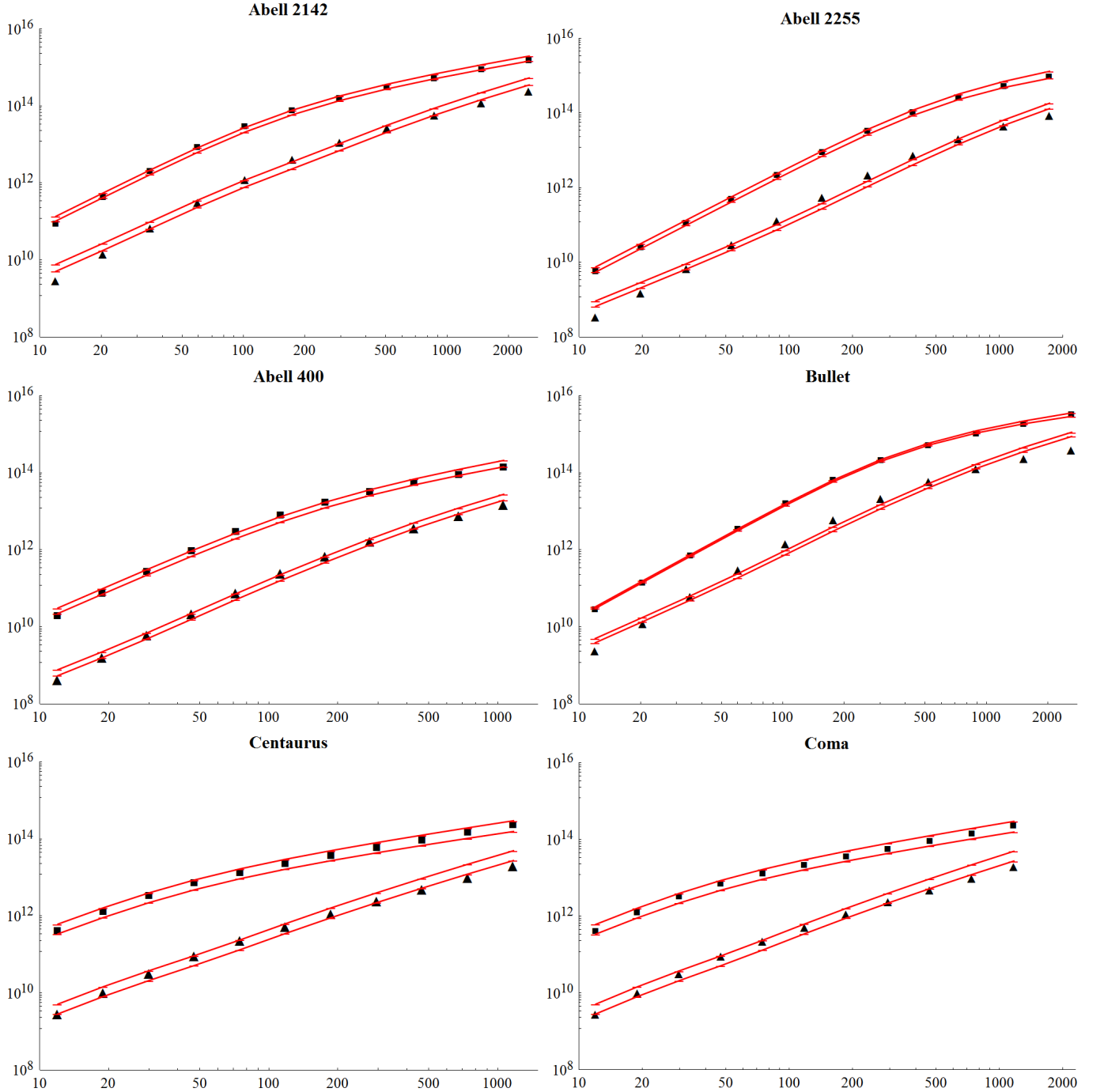


FIG. 6. Log-log plots of MORC and MSTG fits of X-ray cluster mass profiles (compiled from ROSAT and ASCA data). Vertical scale is in solar masses and horizontal scale is in kpc. MORC is increasing the gas mass (triangles) to fit the dynamic mass (squares). MSTG is decreasing the dynamic mass to fit the gas mass. The sizes of the objects are approximately equal to their errors. MORC fit is the upper pair of lines (connecting fit points) over the squares where line separation corresponds to error. MSTG fit is the lower pair of lines (connecting fit points) over the triangles where line separation corresponds to error. Corresponding numerical results are in Tables III & IV.

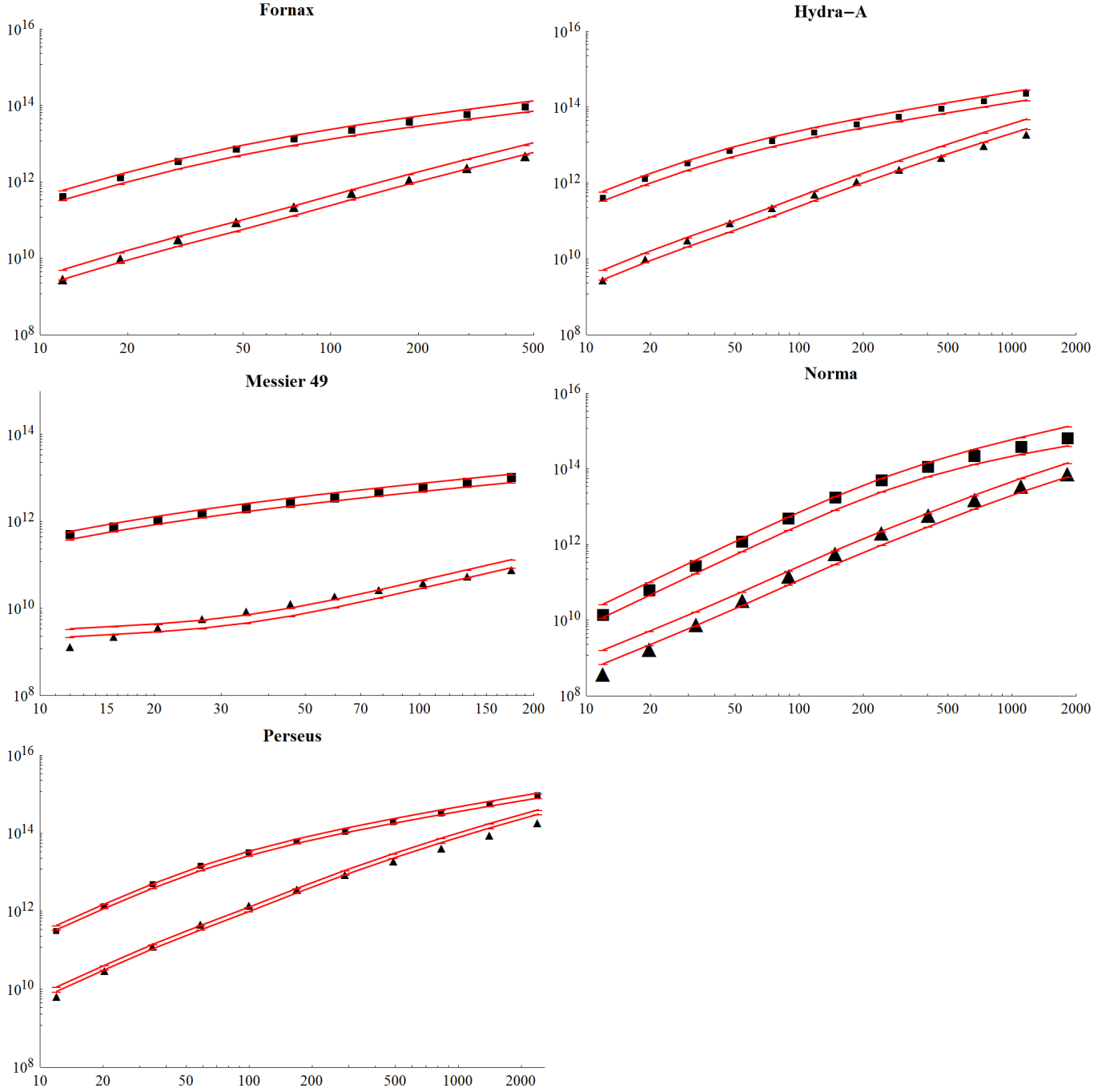


FIG. 7. More log-log plots of MORC and MSTG fits of X-ray cluster mass profiles (compiled from ROSAT and ASCA data). Vertical scale is in solar masses and horizontal scale is in kpc. MORC is increasing the gas mass (triangles) to fit the dynamic mass (squares). MSTG is decreasing the dynamic mass to fit the gas mass. The sizes of the objects are approximately equal to their errors. MORC fit is the upper pair of lines (connecting fit points) over the squares where line separation corresponds to error. MSTG fit is the lower pair of lines (connecting fit points) over the triangles where line separation corresponds to error. Corresponding numerical results are in Tables III & IV.